

AD-773 651

TURBULENT WAKES

Eric Baum

TWR Systems Group  
Redondo Beach, California

31 December 1973

DISTRIBUTED BY:

**NTIS**

**National Technical Information Service**  
**U. S. DEPARTMENT OF COMMERCE**  
5285 Port Royal Road, Springfield Va. 22151

Unclassified

SECURITY CLASSIFICATION OF THIS PAGE (When Data Entered)

REPORT DOCUMENTATION PAGE		READ INSTRUCTIONS BEFORE COMPLETING FORM
1. REPORT NUMBER	2. GOVT ACCESSION NO.	3. RECIPIENT'S CATALOG NUMBER
4. TITLE (and Subtitle)  Turbulent Wakes		5. TYPE OF REPORT & PERIOD COVERED  Final Technical Report
7. AUTHOR(s)  Dr. Eric Baum		6. PERFORMING ORG. REPORT NUMBER 23028-6002-RU-00
9. PERFORMING ORGANIZATION NAME AND ADDRESS TRW Systems Group One Space Park Redondo Beach, California		8. CONTRACT OR GRANT NUMBER(s)  N00014-72-C-0448
11. CONTROLLING OFFICE NAME AND ADDRESS Advanced Research Projects Agency 1400 Wilson Boulevard Arlington, Virginia 22209		10. PROGRAM ELEMENT, PROJECT, TASK AREA & WORK UNIT NUMBERS
14. MONITORING AGENCY NAME & ADDRESS (if different from Controlling Office) Naval Ordnance Laboratory White Oak Silver Spring, Maryland 20910		12. REPORT DATE 31 December 1973
		13. NUMBER OF PAGES
		15. SECURITY CLASS. (of this report)  Unclassified
		15a. DECLASSIFICATION/DOWNGRADING SCHEDULE
16. DISTRIBUTION STATEMENT (of this Report)  Approved for public release, distribution unlimited		
17. DISTRIBUTION STATEMENT (of the abstract entered in Block 20, if different from Report)		
18. SUPPLEMENTARY NOTES		
19. KEY WORDS (Continue on reverse side if necessary and identify by block number) Turbulence modeling Time-dependent Navier-Stokes equations Finite differences Alternating-direction implicit		
20. ABSTRACT (Continue on reverse side if necessary and identify by block number) Summarizes turbulence model equations and finite difference techniques for solving time-dependent compressible turbulent near wake flows. Turbulence properties are described in terms of two variables, the turbulent kinetic energy and an integral length scale. The resulting six partial differential equations are solved using an alternating-direction implicit finite difference method. Solutions are presented for hypersonic flows.		

AD 773 651

23028-6002-RU-00

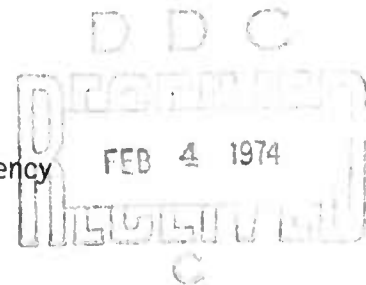
FINAL TECHNICAL REPORT

TURBULENT WAKES

31 December 1973

Principal Investigator: E. Baum (213) 535-2890  
Effective Date of Contract: 1 April 1972  
Expiration Date: 31 December 1973  
Amount of Contract: \$100,000  
Contract Number: N00014-72-C-0448  
Program Code Number: 2E90  
Scientific Officer: Director Fluid Dynamics Programs  
Mathematical and Information Sciences Division  
Office of Naval Research  
Department of the Navy  
Arlington, Virginia 22217

Sponsored by  
Advanced Research Projects Agency  
ARPA Order Number 1801



Approved for public release, distribution unlimited.

The views and conclusions contained in this document are those of the authors and should not be interpreted as necessarily representing the official policies, either expressed or implied, of the Advanced Research Projects Agency of the U.S. Government.

Reproduced by  
NATIONAL TECHNICAL  
INFORMATION SERVICE  
U S Department of Commerce  
Springfield VA 22151

**TRW**  
SYSTEMS GROUP

One Space Park  
Redondo Beach, California 90278

i

## SUMMARY

This report describes a two equation turbulence model and an alternating direction implicit method of solving the mean flow conservation equations and turbulence model equations, with emphasis on application to the calculation of the supersonic near wake behind a slender body. The turbulence model has been shown to adequately predict those low and high speed turbulent flow experiments against which it has been tested. The numerical methods used have demonstrated a particular suitability for the near wake problem because the requirement for locally high spatial resolution does not require a corresponding reduction in temporal step size as in the case of explicit difference methods. Hypersonic near wake results are presented.

## TABLE OF CONTENTS

	<u>Page</u>
1. INTRODUCTION . . . . .	1
2. MODEL EQUATIONS FOR A TURBULENT COMPRESSIBLE FLOW . . . . .	4
3. METHOD OF SOLUTION . . . . .	8
3.1 Variable Spatial Mesh . . . . .	9
3.2 Flux-corrected Transport (FCT) . . . . .	10
3.3 Calculation Sequence . . . . .	13
4. HYPERSONIC NEAR WAKE CALCULATIONS . . . . .	15
4.1 Laminar Hypersonic Near Wake . . . . .	15
4.2 Turbulent Near Wake . . . . .	20
5. CONCLUSIONS . . . . .	24
REFERENCES . . . . .	25

## 1. INTRODUCTION

The principal objective of this program is to develop the capability of performing calculations of turbulent near wakes of slender bodies. Two major subtasks are involved:

1. Develop turbulence model equations applicable to compressible as well as incompressible flows
2. Develop finite difference methods for the solution of the model equations.

Work on the first task has been partially supported by the ROPE Project funded by ABMDA and ARPA under contract DAHC-60-71-C-0049 as well as by the present contract. An integral part of the development of the turbulence model equations is comparison of calculations of simple flows with experiment. Such calculations are necessary to test the validity of the proposed modeling over a sufficiently broad range of conditions as to provide some confidence in their applicability in the near wake of hypersonic slender bodies. These comparisons with experiment can in most cases be made using subsets of the complete time-dependent conservation and turbulence model equations proposed for use in the near wake problem. The particular subset which has been used for this purpose is one which has been applied to the laminar steady calculation of interacting flows,<sup>(1)</sup> and contains both the complete inviscid terms (in the supersonic flow) and boundary-layer-like viscous terms. Since the numerical methods required for the implementation of the model equations in this form had already been developed, this task could be pursued independently of and parallel with that of developing suitable numerical methods for solution of the complete time-dependent equations. The Semi-Annual Technical Report<sup>(2)</sup> contains a preliminary description of the model equations and of the tests of the modeling which had been completed to that date. Further tests have now been completed under the support of the ROPE project, with a complete description presented in Reference 3. Agreement with experiment is now considerably better than was shown in Reference 2. The current version of the model equations will be summarized in the present report. Further testing of the modeling will be continuing under ABMDA support.

The near wake problem, because of the recirculation region immediately behind the body, constitutes a boundary value problem. The proposed computational approach, here, is to obtain the steady flowfield as the asymptotic limit of the time-dependent solution of the Navier-Stokes equations with turbulence modeling. The numerical methods previously applied to related problems have major drawbacks when applied to the calculation of the near wake flowfield at large Reynolds number, related primarily to the fact that the explicit finite difference approximations used required, for stability, that the Courant number  $K_c = (u + c) \frac{\Delta t}{\Delta x}$  be smaller than a limiting value which is of the order unity. (Here,

$u$  = local velocity

$c$  = local sound speed

$\Delta t$  = time increment

$\Delta x$  = local spatial meshsize.)

This limitation is not a serious one for many applications, but proves to be quite wasteful and inefficient when applied to the particular problem of interest, for two related reasons:

1. there are relatively limited flow regions which require much higher spatial resolution than the rest of the domain in order to avoid the generation of unacceptably large spatial truncation errors in these regions; for example, the boundary layer and expansion fan in the neighborhood of the body corner. Since the temporal step size is severely limited, via the Courant condition, by the small spatial meshsizes required in these regions even when the temporal truncation error is quite moderate, the explicit methods can be extremely inefficient.
2. the approach to a steady state occurs in two stages involving separate characteristic times. For arbitrary initial conditions, the flow rapidly develops the familiar near-wake features, including the lip and wake shocks, expansion fan, and a recirculation region. After a time which is of the order of the transit time of a particle across the domain in the outer high speed regions, changes become much slower, and are dictated by the development of the viscous and relatively slow recirculation region. During this final slow approach to a steady state, the explicit methods are still restricted in time step by the stability requirements associated with the smallest spatial mesh in the expansion fan, which has long since ceased to change appreciably with time and hence should not limit the time step for reasons of temporal truncation error.

For these reasons, an implicit finite difference method has been developed which is free of these undesirable stability limitations. This alternating-direction implicit differencing is applied to the conservation form of the equations in order to provide a better description of the flow in the neighborhood of shocks and other regions of large gradient. The general properties of these difference approximations applied to the Navier-Stokes equations were reported in the semi-annual technical report,<sup>(2)</sup> and a description of the method with a number of example applications was presented at the AIAA Computational Fluid Dynamics Conference in Palm Springs,<sup>(4)</sup> July 1973.

These methods have since been applied to the problem of interest, the hypersonic high Reynolds number near wake of a slender body. The remainder of this report is concerned with the description of the application of the general methods described previously to this particular problem, along with the description of special techniques which were found to be required under these particularly difficult conditions, and a presentation of the results of calculations of high Reynolds number hypersonic near wakes. The calculations demonstrate the particular suitability of the method for this type of problem (the Courant number  $K_C$  for these calculations was as large as 20 and was never reduced below 5). The addition of a flux-corrected-transport (FCT) stage to the calculation is shown to permit the description of strong unresolved shocks without the severe numerical difficulties normally associated with dispersive effects which typically appear under these conditions. This is accomplished without resorting to artificial or numerical diffusion which can mask genuine viscous effects which are of interest, and without any increase in the (small) truncation errors associated with the basic difference approximations as previously reported.



## 2. MODEL EQUATIONS FOR A TURBULENT COMPRESSIBLE FLOW

The model being used to represent the non-homogeneous turbulence field in the near wake of a hypersonic body characterizes turbulence properties at each point by two independent variables consisting of the turbulent kinetic energy,  $e = (\overline{u'^2 + v'^2 + w'^2})/2$  and a lateral scale length of the turbulence,  $\lambda$ . To solve for these variables, two partial differential equations are written, each which represents a balance between the production, dissipation, diffusion, and convection of turbulent energy and its rate-of-dissipation. Because of the closure problems always encountered in the Reynolds description of turbulence, the terms appearing in the governing equations are models of the actual processes and are, therefore, approximate. However, reasonable success has been obtained by a number of investigators in the calculation of boundary layers and mixing layers and, consequently optimism exists for the near wake problem. A more rigorous and detailed description of the turbulence which considers its true tensorial character, wherein correlations between all three components of velocity fluctuation as well as orthogonal integral scale lengths obtained from the various spectra are included, could also be applied in principle. However, this approach also suffers from the uncertainties of the closure assumptions, and the additional complexity of many more turbulence variables, constants to be determined, and equations to solve makes it too unwieldy for the near wake problem. The lumped or scalar representation of turbulence by two variables is the simplest representation which contains sufficient generality to be applicable to the problem of interest.

The mean flow equations are altered to account for turbulent diffusion as in Wilcox and Alber. (5)

$$\frac{\partial \rho}{\partial t} + \frac{\partial \rho u}{\partial z} + \frac{1}{r} \frac{\partial}{\partial r} (r \rho v) = 0 \quad \text{continuity}$$

$$\frac{\partial \rho u}{\partial t} + \frac{\partial}{\partial z} [\rho u^2 - \sigma_{zz} + p] + \frac{1}{r} \frac{\partial}{\partial r} [r (\rho uv - \sigma_{rz})] = 0 \quad \text{axial momentum}$$

$$\frac{\partial \rho v}{\partial t} + \frac{\partial}{\partial z} [\rho u v - \sigma_{rz}]$$

radial momentum

$$+ \frac{1}{r} \frac{\partial}{\partial r} [r (\rho v^2 - \sigma_{rr})] + \frac{\partial P}{\partial r} = - \frac{\sigma_{\theta\theta}}{r}$$

$$\frac{\partial \rho E}{\partial t} + \frac{\partial}{\partial z} [\rho u H + q_z - u \sigma_{zz} - v \sigma_{rz}]$$

total energy

$$+ \frac{1}{r} \frac{\partial}{\partial r} [r (\rho v H + q_r - u \sigma_{rz} - v \sigma_{rr})] = 0$$

where

$$\sigma_{zz} = \frac{1}{Re} \left\{ 2\mu \frac{\partial u}{\partial z} + \lambda \left[ \frac{\partial u}{\partial z} + \frac{1}{r} \frac{\partial}{\partial r} (rv) \right] \right\}$$

$$\sigma_{rr} = \frac{1}{Re} \left\{ 2\mu \frac{\partial v}{\partial r} + \lambda \left[ \frac{\partial u}{\partial z} + \frac{1}{r} \frac{\partial}{\partial r} (rv) \right] \right\}$$

$$\sigma_{\theta\theta} = \frac{1}{Re} \left\{ 2\mu \frac{v}{r} + \lambda \left[ \frac{\partial u}{\partial z} + \frac{1}{r} \frac{\partial}{\partial r} (rv) \right] \right\}$$

$$\sigma_{rz} = \frac{\mu}{Re} \left\{ \frac{\partial u}{\partial r} + \frac{\partial v}{\partial z} \right\}$$

$$q_z = - \frac{1}{Re} \left( \frac{\mu}{Pr} \right) \frac{\partial h}{\partial z}$$

$$q_r = - \frac{1}{Re} \left( \frac{\mu}{Pr} \right) \frac{\partial h}{\partial r}$$

All quantities are here non-dimensionalized with reference length  $L$ , velocity  $u_r$ , density  $\rho_r$ , and laminar viscosity  $\mu_r$ . Pressure is normalized with  $\rho_r u_r^2$  and enthalpy with  $u_r^2$ .  $E$  is total energy ( $H - P/\rho$ ) and  $H$  is total enthalpy ( $h + \frac{u^2}{2} + \frac{v^2}{2}$ ). Turbulence is included in the stress and heat transfer terms through the definitions of the transport properties:

$$\mu = \mu^L + \mu^T \quad \text{where } \mu^T = \rho e^{1/2} L Re$$

$$\left(\frac{\mu}{Pr}\right) = \left(\frac{\mu}{Pr}\right)^L + \left(\frac{\mu}{Pr}\right)^T$$

where  $e$  is normalized by  $u_r^2$  and  $\lambda$  by  $L$ .

The governing equations for  $e$  and  $\lambda$  are the turbulent kinetic energy equation and an equation for the rate-of-dissipation,  $\epsilon_d = C_d e^{3/2}/\lambda$  where  $C_d$  is a constant. The first equation has been used for incompressible flows in various modern investigations, beginning with Bradshaw<sup>(6)</sup> and is reasonably well understood and accepted. Less agreement exists with respect to the second turbulence modeling equation, and the dissipation rate equation based on the work of Harlow and Nakayama<sup>(7)</sup> and Jones and Launder<sup>(8)</sup> was chosen after comparative studies showed that this formulation agrees most favorably with compressible and incompressible boundary layer experiments (see References 2 and 3).

The turbulence model equations in the appropriate coordinates are:

$$\begin{aligned} & \frac{\partial \rho e}{\partial t} + \frac{\partial}{\partial z} \left[ \rho u e - \frac{\mu^L}{Re} \frac{\partial e}{\partial z} - \frac{S_1}{Re} \frac{\mu^T}{\rho} \frac{\partial e \rho}{\partial z} \right] \\ & + \frac{1}{r} \frac{\partial}{\partial r} \left[ r \left( \rho v e - \frac{\mu^L}{Re} \frac{\partial e}{\partial r} - \frac{S_1}{Re} \frac{\mu^T}{\rho} \frac{\partial e \rho}{\partial r} \right) \right] \\ & - \epsilon_1 \frac{\rho e u}{\rho a^2} \frac{\partial P}{\partial z} - \epsilon_1 \frac{\rho e v}{\rho a^2} \frac{\partial P}{\partial r} \qquad \text{turbulence energy} \\ & - \mu^T \left[ 2 \left( \frac{\partial v}{\partial r} \right)^2 + 2 \left( \frac{v}{r} \right)^2 + 2 \left( \frac{\partial u}{\partial z} \right)^2 + \left( \frac{\partial v}{\partial z} + \frac{\partial u}{\partial r} \right)^2 \right] \\ & - \lambda^T \left( \frac{1}{r} \frac{\partial r v}{\partial r} + \frac{\partial u}{\partial z} \right)^2 = - \rho \epsilon - \frac{\pi}{4 C_D^2 Re} \left( \frac{\mu^L}{e^2} \epsilon^2 \right) \end{aligned}$$

$$\begin{aligned}
& \frac{\partial \rho \epsilon}{\partial t} + \frac{\partial}{\partial z} \left[ \rho u \epsilon - \frac{\mu}{\text{Re}} \frac{\partial \epsilon}{\partial z} - \frac{S_2}{\text{Re}} \frac{\mu^T}{\rho^{3/2}} \frac{\partial \epsilon \rho^{3/2}}{\partial z} \right] \\
& + \frac{1}{r} \frac{\partial}{\partial r} \left[ r \left( \rho v \epsilon - \frac{\mu}{\text{Re}} \frac{\partial \epsilon}{\partial r} - \frac{S_2}{\text{Re}} \frac{\mu^T}{\rho^{3/2}} \frac{\partial \epsilon \rho^{3/2}}{\partial r} \right) \right] \\
& - \xi_2 \frac{\epsilon u}{a^2} \frac{\partial P}{\partial z} - \xi_2 \frac{\epsilon v}{a^2} \frac{\partial P}{\partial r} \quad \text{dissipation rate} \\
& - C_1 \frac{\epsilon}{e} \left\{ \mu^T \left[ 2 \left( \frac{\partial v}{\partial r} \right)^2 + 2 \left( \frac{v}{r} \right)^2 + 2 \left( \frac{\partial u}{\partial z} \right)^2 + \left( \frac{\partial v}{\partial z} + \frac{\partial u}{\partial r} \right)^2 \right] \right. \\
& \left. + \lambda^T \left( \frac{1}{r} \frac{\partial r v}{\partial r} + \frac{\partial u}{\partial z} \right)^2 \right\} = - C_2 \rho \frac{\epsilon^2}{e} - \frac{17\pi}{40 C_D^2} \frac{\mu^L \epsilon^3}{\text{Re} e^3}
\end{aligned}$$

where  $\epsilon \equiv C_D e^{3/2} / \ell$  so that  $\mu^T = \rho C_D e^2 \text{Re} / \epsilon$

$$S_1 = 1.0, \quad S_2 = 0.77, \quad \xi_1 = 1, \quad \xi_2 = 2.5,$$

$$C_D = .09, \quad C_1 = 1.41, \quad C_2 = 1.89, \quad \text{Pr}^T = 0.9$$

$a$  = local sound speed.

The laminar sublayer dissipation terms in the turbulence equations (described in References 2 and 3 where they are applied in the compressible boundary layer calculations used to verify the compressibility modeling of the diffusion terms in these equations) have not been included here since resolution of the sublayer on the body base-wall will not be attempted.

### 3. METHOD OF SOLUTION

The TACIT alternating-direction-implicit differencing method described in detail in References 2 and 4 has been modified slightly to improve its performance at high Reynolds number, when poor resolution in regions of large gradient introduces an associated large spatial truncation error. Since the method contains no direct numerical or artificial diffusion to damp out such truncation-error-induced oscillatory disturbances, they may become large enough to violate the requirement of positive static temperature and terminate the calculation. The most direct way of avoiding these problems is to provide adequate spatial resolution everywhere. When mesh spacing is uniform, this is not practical at large Reynolds number since the mesh spacing required to resolve the boundary layers and the expansion region near the body corner is so small that the calculation becomes unreasonably costly in computer storage and time. A second approach is to use a variable mesh spacing, with fine spatial resolution used only where required. This requires some modification of the differencing presented in References 2 and 4.

The variable mesh capability alone does not completely eliminate the problems associated with local inadequate spatial resolution at high Reynolds number, since one does not always know in advance where all of the problem areas will occur. For instance, internal shocks such as the lip and wake shocks in the near wake cannot be precisely located a priori. For this reason, a differencing technique introduced by Boris and Book<sup>(9)</sup> which they term Flux-corrected Transport (FCT) has been incorporated into TACIT. This technique consists basically of introducing an artificial diffusion into the conservation equations which prevents overshoots which would otherwise be generated by large local truncation errors. Then, in a subsequent step, the effect of this artificial diffusion is removed identically everywhere except at those few points where this would create a new extremum. At these points, the diffusive flux used in removing the effect of the artificial diffusion is limited in such a way that the new extremum is not formed,

while still satisfying overall conservation. The details of the FCT algorithm incorporated into a variable mesh version of TACIT will be described in Section 3.2.

### 3.1 Variable Spatial Mesh

The terms whose difference approximations are affected by the use of a variable mesh are of the general form  $\frac{\partial}{\partial x} f$  and  $\frac{\partial}{\partial x} g \frac{\partial h}{\partial x}$ . When these terms are evaluated at meshpoint  $i$  (corresponding to the spatial location  $x_i$ ) the difference approximations used are:

$$\frac{\partial f}{\partial x} = D^- f_{i+1} + (D^+ - D^-) f_i - D^+ f_{i-1}$$

where, if  $f = g \frac{\partial h}{\partial x}$

$$f_{i+1} = g_{i+1} \left\{ (D - D^+) h_{i+1} - D h_i + D^+ h_{i-1} \right\}$$

$$f_{i-1} = g_{i-1} \left\{ -D^- h_{i+1} + D h_i - (D - D^-) h_{i-1} \right\}$$

$$f_i = g_i \left\{ D^- h_{i+1} + (D^+ - D^-) h_i - D^+ h_{i-1} \right\}$$

where

$$D^+ = \frac{x_{i+1} - x_i}{(x_{i+1} - x_{i-1})(x_i - x_{i-1})}$$

$$D = \frac{x_{i+1} - x_{i-1}}{(x_{i+1} - x_i)(x_i - x_{i-1})}$$

$$D^- = \frac{x_i - x_{i-1}}{(x_{i+1} - x_{i-1})(x_{i+1} - x_i)}$$

These general expressions replace those which are presented in References 2 and 4 for the special case of uniform mesh spacing. With these approximations, inviscid terms retain their second order accuracy (truncation error of order  $(\Delta x)^2$ ) while diffusion terms are functionally second order accurate provided  $\Delta x$  changes sufficiently slowly from point to point.

### 3.2 Flux-corrected Transport (FCT)

The FCT algorithm improves the behavior of the finite difference solution in regions where gradients are large and changing rapidly. In these regions, the truncation errors of the difference approximations become large. If the regions are thin (such as in a shock or thin shear layer) and the difference approximations are conservative, so that overall conservation across the thin region is maintained, these local truncation errors may not be of great concern. They become important, however, if the errors propagate away from their region of origin in the form of wave-like disturbances and, from a practical standpoint, these errors may cause the calculation to fail if they produce oscillations of amplitude large enough to violate a physical limit to the range of a variable (i.e.,  $T < 0$  or  $P < 0$ ). The FCT algorithm adds a large artificial diffusive terms to the conservation equations to ensure that oscillatory overshoots of this type do not occur. The effect of this diffusive term is then removed in a second calculation step. In the absence of any "corrections", the net effect of these two steps is identical to that of a one step calculation in which the artificial diffusion term is omitted. A "correction" is introduced during the step which removes the diffusive term, but only if the effect of this operation is to introduce a new extremum in the diffused quantity. If a correction is required, it is imposed in conservation form (that is, if the diffusive flux leaving a volume element is reduced as a result of the correction, the corresponding flux entering the adjacent element is correspondingly reduced to maintain overall conservation). "Corrections" are required only in those local regions of very large spatial truncation error where the magnitude of the truncation error is not of great concern since one only expects correct overall conservation across such spatially unresolved regions. The truncation errors associated with the corrections are therefore irrelevant as long as overall conservation is maintained. Within this general framework describing the

FCT algorithm, there are many alternative detailed formulations, of which the following has been implemented in the TACIT code.

$$\frac{\partial A}{\partial t} + \frac{\partial uA}{\partial z} + \dots = \frac{2(\phi_{i+1/2} - \phi_{i-1/2})}{(z_{i+1} - z_{i-1})} + \frac{2(\phi_{j+1/2} - \phi_{j-1/2})}{r(r_{j+1} - r_{j-1})}$$

where

$$\phi_{i+1/2} = \frac{\alpha}{2\Delta t} (z_{i+1} - z_{i-1})(A_{i+1} - A_i)$$

$$\phi_{i-1/2} = \frac{\alpha}{2\Delta t} (z_{i+1} - z_{i-1})(A_i - A_{i-1})$$

$$\phi_{j+1/2} = \frac{\alpha r}{2\Delta t} (r_{j+1} - r_{j-1})(A_{j+1} - A_j)$$

$$\phi_{j-1/2} = \frac{\alpha r}{2\Delta t} (r_{j+1} - r_{j-1})(A_j - A_{j-1})$$

The artificial diffusion terms on the right are differenced explicitly or implicitly, consistent with the other spatial difference approximations being used. The artificial diffusion terms can be considered as approximation of terms of the form  $\frac{\partial}{\partial t} (D_1 \frac{\partial A}{\partial z}) + \frac{1}{r} \frac{\partial}{\partial r} (r D_2 \frac{\partial A}{\partial r})$ . The diffusivities  $D_1$  and  $D_2$  are functions of position and are defined in such a way as to make the final difference approximation as simple as possible. The diffusion terms are removed by means of the following step:

$$A = \bar{A} - \frac{2(\bar{\phi}_{i+1/2} - \bar{\phi}_{i-1/2})\Delta t}{(z_{i+1} - z_{i-1})} - \frac{2(\bar{\phi}_{j+1/2} - \bar{\phi}_{j-1/2})\Delta t}{r(r_{j+1} - r_{j-1})}$$

where  $\bar{A}$  is the value obtained when the diffusion term was included in the conservation equation. Flux terms  $\phi$  are evaluated at time levels such that the terms are identically removed in the absence of flux corrections. The corrected flux terms  $\bar{\phi}$  are evaluated as follows:



$$\bar{\phi}_{i+1/2} = \text{sgn } \phi_{i+1/2} \max \left\{ 0, \min \left[ \frac{(z_{i+1} - z_{i-1})}{2\Delta t} (A_i - A_{i-1}) \text{sgn } \phi_{i+1/2}, \right. \right. \\ \left. \left. |\phi_{i+1/2}|, \frac{(z_{i+1} - z_{i-1})}{2\Delta t} (A_{i+2} - A_{i+1}) \text{sgn } \phi_{i+1/2} \right] \right\}$$

$$\bar{\phi}_{i-1/2} = \text{sgn } \phi_{i-1/2} \max \left\{ 0, \min \left[ \frac{(z_{i+1} - z_{i-1})}{2\Delta t} (A_{i-1} - A_{i-2}) \text{sgn } \phi_{i-1/2}, \right. \right. \\ \left. \left. |\phi_{i-1/2}|, \frac{(z_{i+1} - z_{i-1})}{2\Delta t} (A_{i+1} - A_i) \text{sgn } \phi_{i-1/2} \right] \right\}$$

$$\bar{\phi}_{j+1/2} = \text{sgn } \phi_{j+1/2} \max \left\{ 0, \min \left[ \frac{r}{2\Delta t} (r_{j+1} - r_{j-1})(A_j - A_{j-1}) \text{sgn } \phi_{j+1/2}, \right. \right. \\ \left. \left. |\phi_{j+1/2}|, \frac{r}{2\Delta t} (r_{j+1} - r_{j-1})(A_{j+2} - A_{j+1}) \text{sgn } \phi_{j+1/2} \right] \right\}$$

$$\bar{\phi}_{j-1/2} = \text{sgn } \phi_{j-1/2} \max \left\{ 0, \min \left[ \frac{r}{2\Delta t} (r_{j+1} - r_{j-1})(A_{j-1} - A_{j-2}) \text{sgn } \phi_{j-1/2}, \right. \right. \\ \left. \left. |\phi_{j-1/2}|, \frac{r}{2\Delta t} (r_{j+1} - r_{j-1})(A_{j+1} - A_j) \text{sgn } \phi_{j-1/2} \right] \right\}$$

where  $\text{sgn } \phi$  denotes "the sign of  $\phi$ ". These tests constrain the change in  $A$  due to the removal of the diffusion term in such a way that  $A$  can at most be made to equal the values at adjacent meshpoints, but cannot overshoot these values. Except in very local regions, these tests do not result in corrections, so that almost everywhere,  $\bar{\phi} = \phi$ .

### 3.3 Calculation Sequence

For purposes of illustration, we define the following sequence of time steps:



At the start of the calculation, we assume that initial conditions in  $P$ ,  $U$ ,  $V$ , and  $H$  are specified at  $t = t_1$ . Initial values of the turbulence properties  $e$  and  $\epsilon$  are assumed known at  $t = t_{3/2}$ . The calculation proceeds as follows:

1. The mean flow equations are solved over the interval  $t_1 \rightarrow t_2$  using "odd-step" differencing ( $z$  derivatives differenced implicitly at  $t_2$ ,  $r$  derivatives differenced explicitly at  $t_1$ , except for  $e$  and  $\epsilon$  which are evaluated at  $t_{3/2}$ )
2. The turbulence equations are solved over the interval  $t_{3/2} \rightarrow t_{5/2}$  using "odd-step" differencing ( $z$  derivatives differenced implicitly at  $t_{5/2}$ ,  $r$  derivatives differenced explicitly at  $t_{3/2}$ , except for mean flow properties  $P$ ,  $U$ ,  $V$ ,  $H$  which are evaluated at  $t_2$ )
3. The mean flow equations are solved over the interval  $t_2 \rightarrow t_3$  using "even-step" differencing ( $z$  derivatives differenced explicitly at  $t_2$ ,  $r$  derivatives differenced implicitly at  $t_3$ , except for  $e$  and  $\epsilon$  which are evaluated at  $t_{5/2}$ )
4. The turbulence equations are solved over the interval  $t_{5/2} \rightarrow t_{7/2}$  using "even-step" differencing ( $z$  derivatives differenced explicitly at  $t_{3/2}$ ,  $r$  derivatives differenced implicitly at  $t_{5/2}$ , except for mean flow properties which are evaluated at  $t_3$ .)

The calculation continues, using steps 1-2 if  $K$  is odd, 3-4 if  $K$  is even. The generation, dissipation and pressure gradient terms in the turbulence equations, which do not involve gradients of the turbulence variables, are

evaluated as average values over the time interval (half implicit, half explicit). For  $\Delta t$  constant, the entire calculation sequence maintains second order accuracy in both spatial and temporal increments. The split time interval for mean flow and turbulence variables is used for computational efficiency, since it permits the sequential solution of (1) the coupled mean flow equations and then (2) the coupled turbulence equations, rather than requiring the simultaneous solution of all six coupled equations. The sequential solution involves the solution of large numbers of coupled algebraic equations of diagonal band form with a band width for step (1) of 15 elements and a width for step (2) of 7 elements. The simultaneous solution of all equations requires a band width of 22 elements. Since the Gaussian elimination method used to solve the equations requires computing time proportional to  $m^2 + 3m$  (where  $m$  is the number of elements to the left or right of the diagonal, whichever is smaller), the sequential solution requires only 25% more computing time than a laminar calculation, while the simultaneous solution would require 85% more.

An additional advantage of the sequential method of solution arises in flow situations where the turbulence equations are dominated by generation, dissipation and/or pressure gradient terms. Under those conditions, the mean flow equations require very few iterations before the solution of the linearized equations converges to that of the non-linear finite difference equations. The turbulence equations may require many more iterations, but in the sequential method, each iteration of the turbulence equations takes only 25% of the time of an iteration of the mean flow equations. The net savings are very substantial.

It should be noted, here, that the above situation (in which generation, dissipation and/or pressure gradient terms dominate) is analogous to chemically reacting flow calculations in which a local equilibrium is being approached, i.e., the equations become stiff and hence unstable when solved using explicit difference methods unless extremely small time increments are used. The implicit method used here has no difficulties under those conditions, and, in fact, can obtain an exact "equilibrium" solution (in which convection and diffusion terms, including the time derivative term, are identically zero) if reasonably accurate initial estimates are provided.

## 4. HYPERSONIC NEAR WAKE CALCULATIONS

The turbulence modeling and structure of the TACIT code, as described in Sections 2 and 3.3, combine to uncouple the calculation of the turbulence properties from the calculation of the mean flow variables. That is, the mean flow calculation for a turbulent flow differs from that for a laminar flow only in the viscosity law and Prandtl number, and the turbulence contribution to total viscosity is constant over any given mean flow calculation time interval. This permits the turbulent mean flow calculation procedure to be completely checked out independently of the turbulence model equations by simply specifying a laminar viscosity law.

### 4.1 Laminar Hypersonic Near Wake

The test case used for preliminary calculations (using the uniform spatial mesh version of the code) was an 8 degree sharp cone with a shoulder rounded to a radius  $r/D_{\text{base}} = 1/12$ ,  $M_{\infty} = 21$ ,  $Re_{\infty D} = 2.5 \times 10^5$ , with a cold wall ( $H_w/H_{\infty} = .02$ ). The viscosity law used was  $\mu/\mu_{\infty} = T/T_{\infty}$ , with  $Pr = 1$ . The flow around the corner, from an initial 8 degree wall inclination to the point where the wall inclination is -29 degrees, was calculated using the steady state code of Reference 1.

This calculation could not be made to reach a steady state without encountering a state in which  $T < 0$  in a local region associated with the wake of the outer edge of the boundary layer. The problem is associated with the large spatial truncation errors generated in this region of large and poorly resolved gradients. The initial boundary layer profiles at the body corner were then rescaled to make the boundary layer thicker by a factor of five to provide a less severe test case. When problems still persisted, the program was rewritten to provide a variable spatial mesh. Using the mesh shown in Figure 1, behavior was considerably improved, but again  $T < 0$  was eventually encountered in the wake of the outer edge of the boundary layer as it passes through the corner expansion fan. The incorporation of the FCT algorithm finally eliminated this problem and a smooth approach to steady state was obtained.

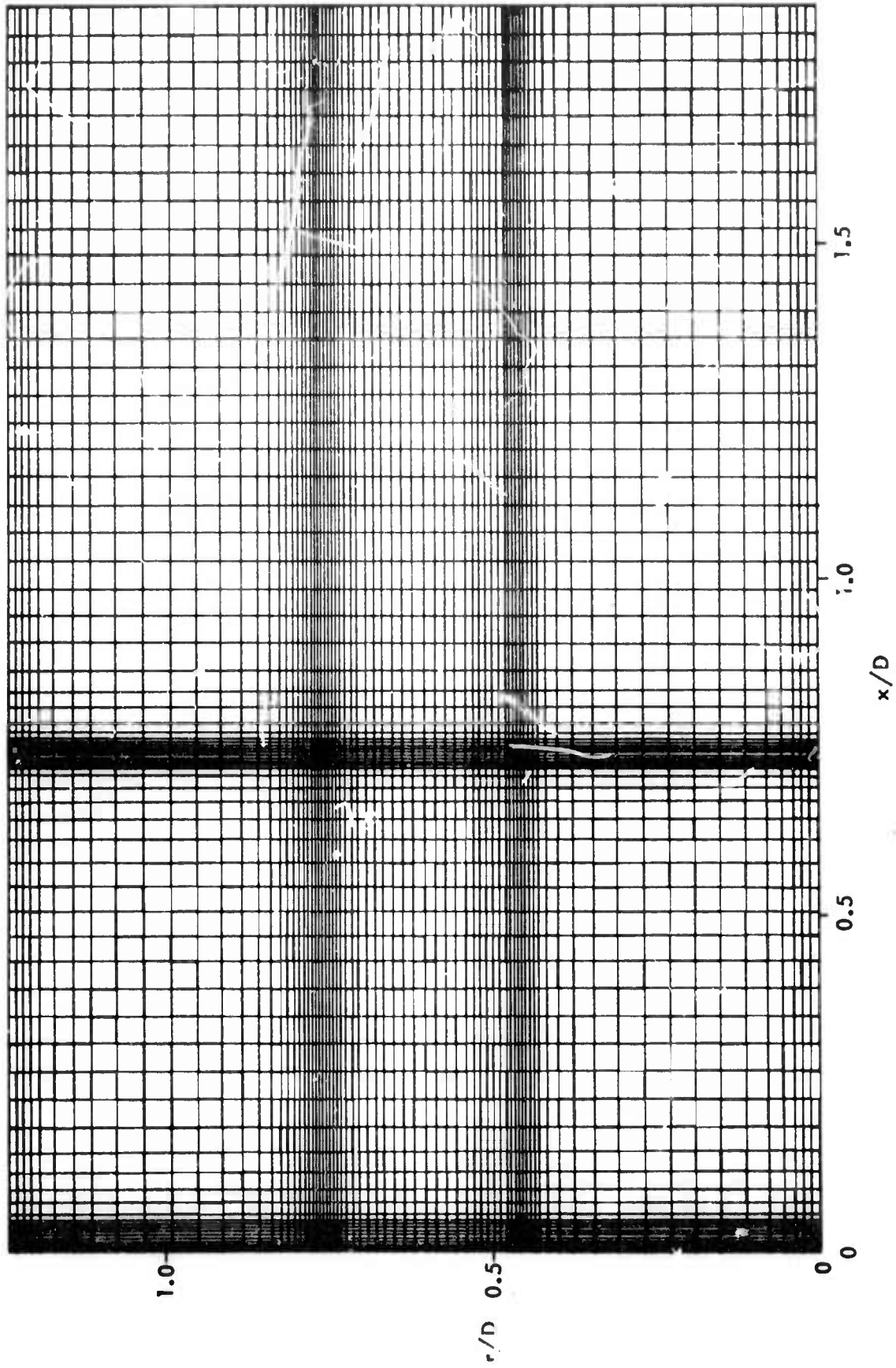


Figure 1. Computation Mesh for Hypersonic ( $M_\infty = 21$ ) Near Wake Calculation

The boundary conditions for this calculation were:

a) left-hand boundary

1) on base wall:  $u = v = 0$ ,  $H = H_w$ ,  $P$  from continuity

2) above corner:  $u$ ,  $v$ ,  $H$ ,  $T$  specified

b) upper boundary: outflow ( $u$ ,  $v$ ,  $H$ ,  $P$  extrapolated)

c) right-hand boundary: outflow

d) lower (axis) boundary:  $\frac{\partial u}{\partial r} = \frac{\partial P}{\partial r} = \frac{\partial H}{\partial r} = 0$ ,  $v = 0$ .

A map of the computed static pressure is presented in Figure 2. At the outer (large  $r/D$ ) edge of the domain, the expansion fan can be seen to have an anomalous structure. This is due to an approximation used in specifying the inflow boundary conditions above the body shoulder; i.e., the inviscid flow outside the boundary layer was taken to be a uniform flow corresponding to wall conditions for a Taylor-Maccoll inviscid cone flow-field. Since the Mach angle is smaller than the flow inclination angle in this high Mach number flow region, the disturbance is carried upward and actually leaves the domain through the upper boundary. Unless the calculation is carried much further downstream, where the outer streamlines are turned inwards by the expansion fan and the influence of this outer region finally becomes felt near the axis, the discrepancies in the outer region are of no consequence.

With the thick initial boundary layer used in this test case, the lip shock does not appear as a separately identifiable structure. The lip-wake shock has its origin in the pressure gradients generated in the recirculation region, and is further strengthened by the increasing pressure in the near wake, to a point about  $0.5 X/D$  downstream of the base wall. At this point of maximum pressure,  $P/P_\infty \approx 3$  at the centerline. The favorable pressure gradient downstream of this point rapidly weakens the wake shock.

The corresponding static temperature map is shown in Figure 3. Since the body wall is cold, the boundary layer temperature has a maximum value at a point well removed from the wall. The decrease in temperature of the wake of this part of the boundary layer as it passes through the corner



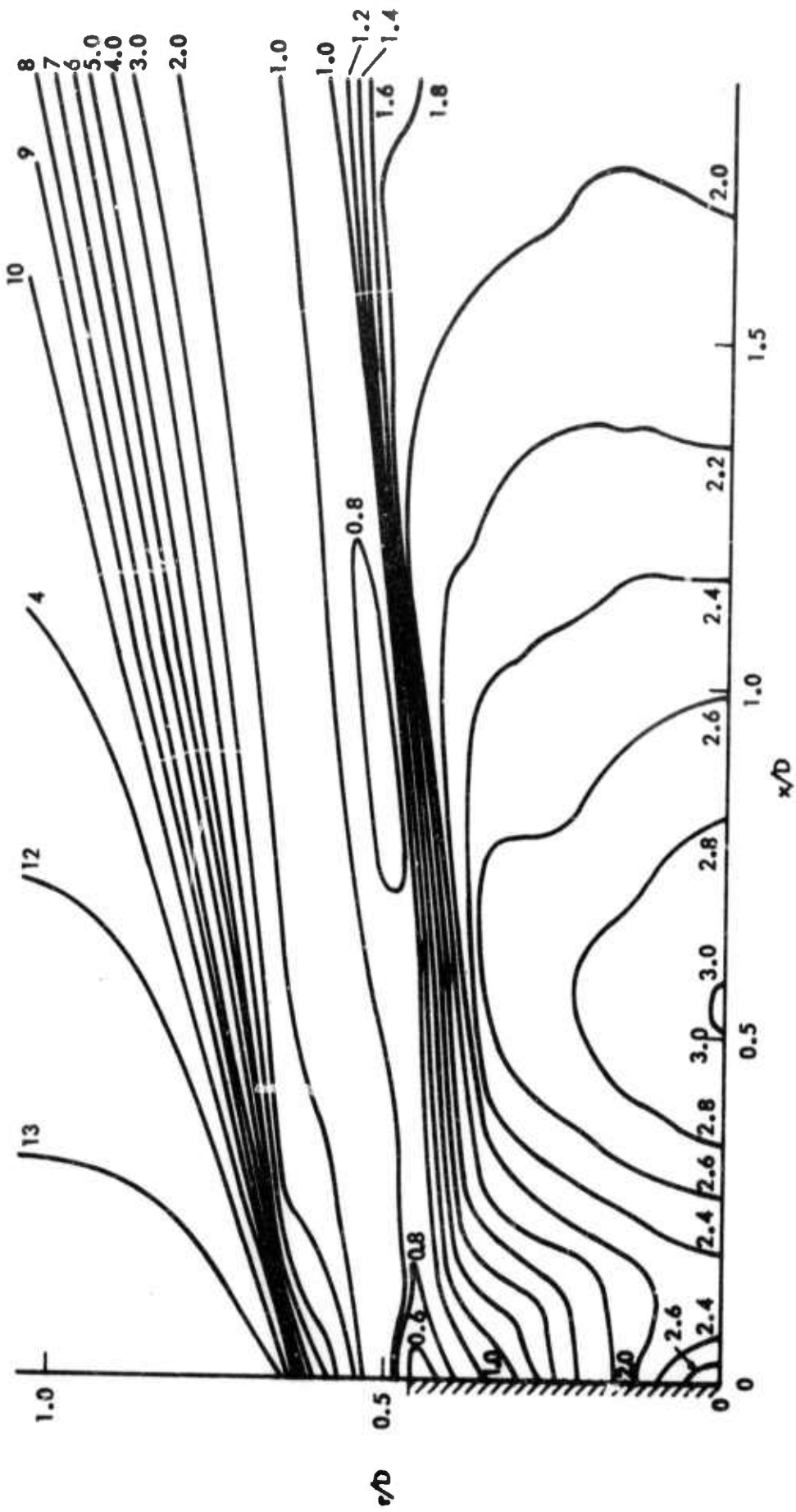


Figure 2. Static Pressure  $P/P_\infty$ :  $M_\infty = 21$ ,  $Re_{\infty D} = 2.5 \times 10^5$ ,  $H_w/H_\infty = 0.02$

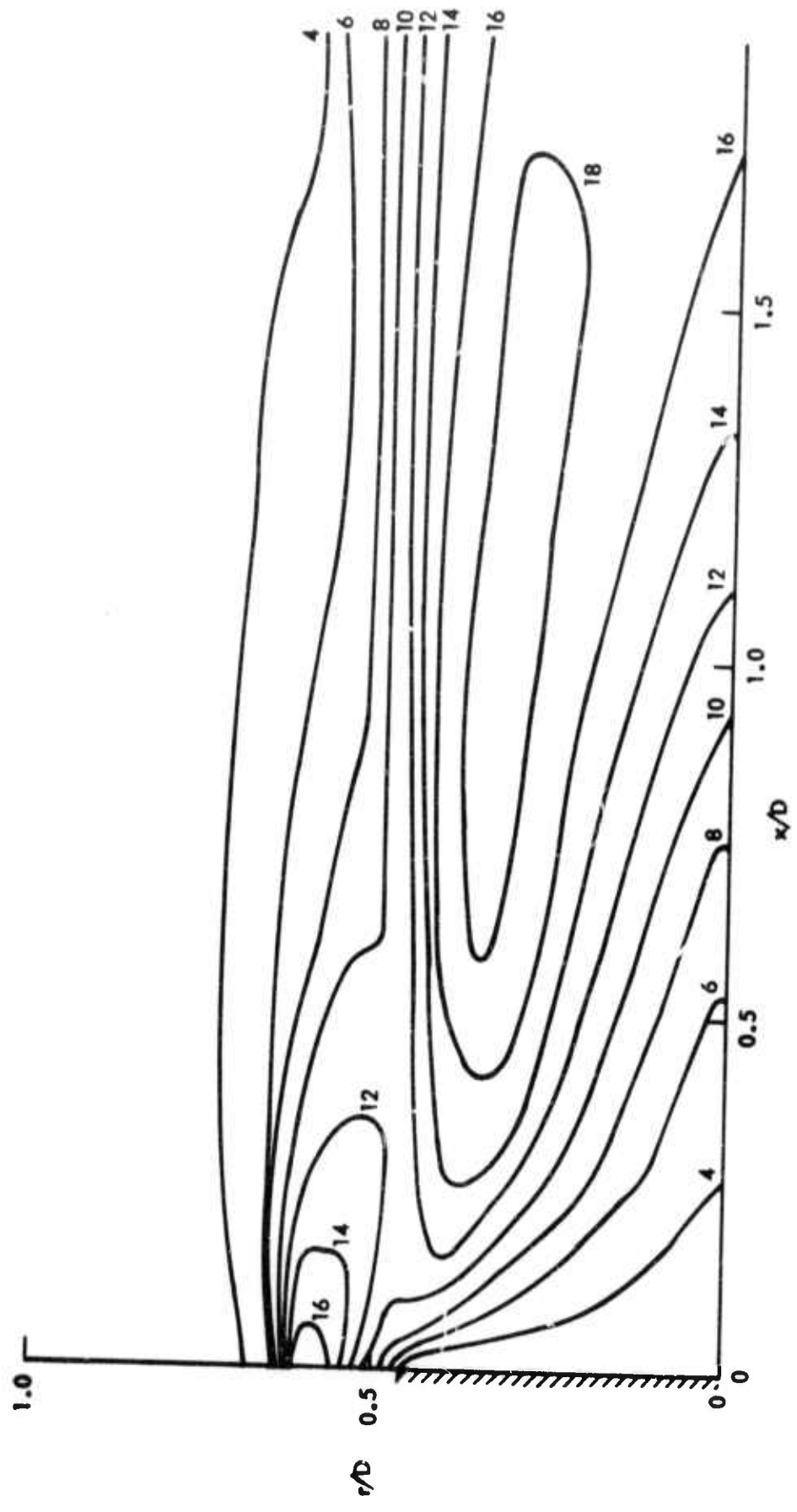


Figure 3. Static Temperature  $T/T_\infty$ :  $M_\infty = 21$ ,  $Re_{\infty D} = 2.5 \times 10^5$ ,  $H_w/H_\infty = 0.02$



expansion fan is evident in the figure. The region of peak temperature reappears after crossing the wake shock, but the peak is slowly eroded by diffusion to cooler surrounding gas at the same time the flow nearer the axis is being heated by dissipation. At the downstream end of the domain, the static temperature has become almost uniform below the shock.

A corresponding map of flow speed  $q/u_\infty$  is shown in Figure 4. Separation occurs on the base wall slightly below the "corner". Remembering that a steady code was used to compute the flow around the rounded body shoulder to a point where the wall inclination is -29 degrees (the estimated separation point), this indicates that this estimated inclination angle was too small by several degrees. The velocities in the recirculation region are quite small, due to the combination of large  $Re$  and thick boundary layer. The thin boundary layer on the base wall is evident from the .01 velocity contour.

Figure 5 shows contours of total enthalpy. Again, the total enthalpy in the recirculation region remains quite small because of the combination of slow diffusion (large  $Re$ ) and small gradients (thick boundary layer). The convergence of total enthalpy contours to the axis downstream of the wake stagnation point is due to a combination of the necking down of the streamlines due to the rapidly increasing axial mass flux near the axis, and the effects of diffusion and dissipation.

#### 4.2 Turbulent Near Wake

A calculation has been initiated under turbulent flow conditions, corresponding to an experimental investigation by Gran<sup>(10)</sup>. The body is a sharp three degree half angle adiabatic cone with a rounded shoulder ( $r/D_{\text{cone}} = 1/12$ ),  $M_\infty = 7.56$ ,  $Re_{\infty D} = 1.7 \times 10^6$ . The inflow boundary conditions are obtained, as in the preceding laminar case, by performing a steady flow calculation expanding the boundary layer around the corner to a wall inclination of -28°. The initial conditions for this calculation are obtained by starting with estimated profiles approximately two base diameters upstream of the shoulder and computing the development of mean flow and turbulence properties along the body. Comparison with the measured velocity profile

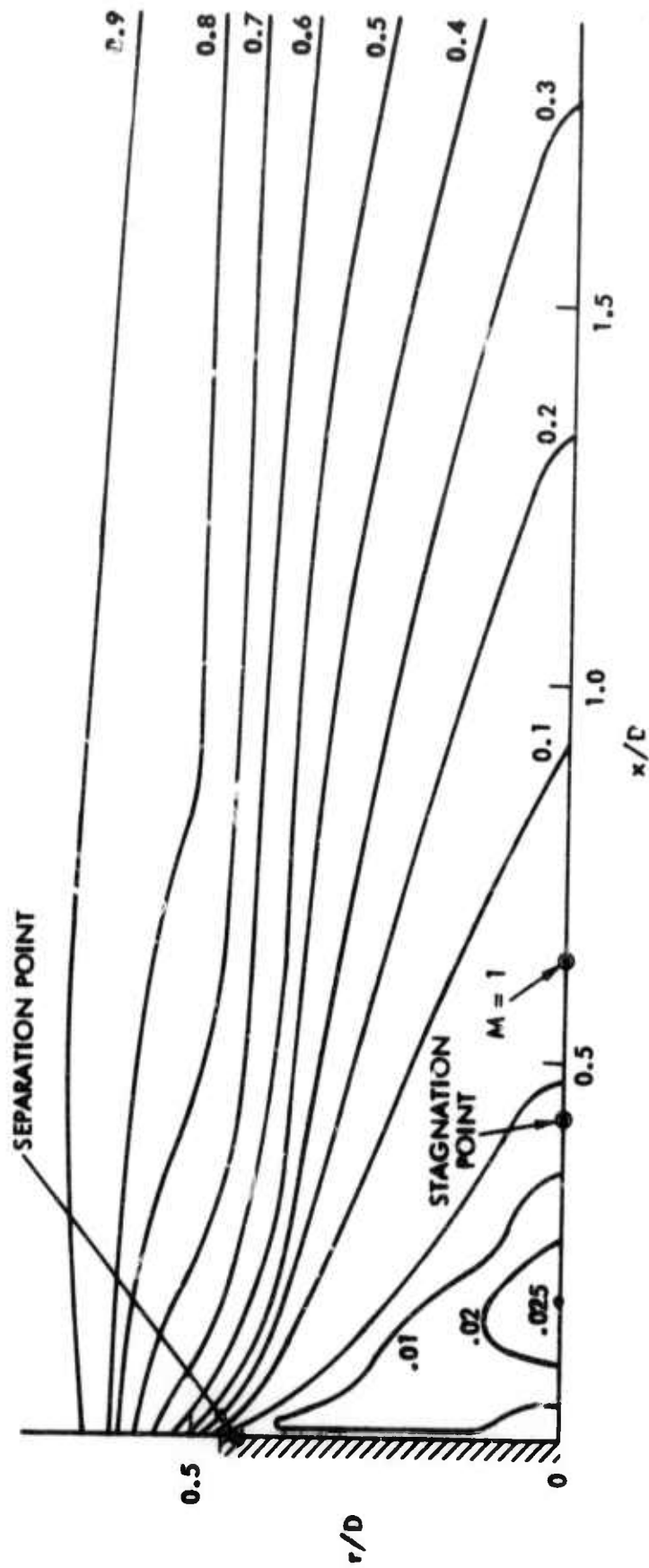


Figure 4. Flow Speed  $q/u_\infty$ :  $M = 21$ ,  $Re_{\infty D} = 2.5 \times 10^5$ ,  $H_w/H_\infty = 0.02$

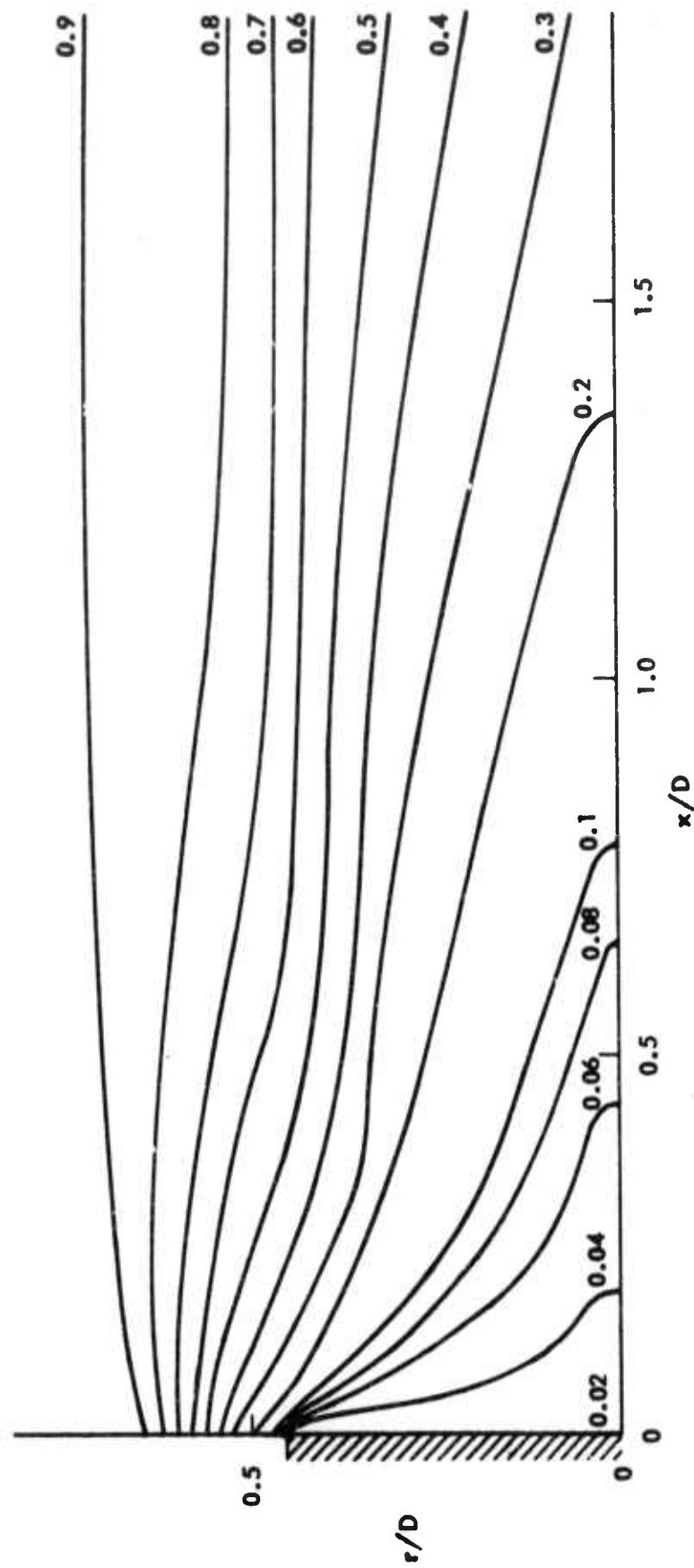


Figure 5. Total Enthalpy  $H/H_\infty$ :  $M_\infty = 21$ ,  $Re_{\infty D} = 2.5 \times 10^5$ ,  $H_w/H_\infty = 0.02$

at the corner shows acceptable agreement. The initial values of the dependent variables are specified arbitrarily, with the objective of maintaining compatibility with the boundary conditions throughout the calculation, i.e., the flow must never reverse and come in through an outflow boundary and should preferably remain always supersonic with respect to this boundary. Initial turbulence properties are specified to make the turbulence energy and the turbulent viscosity small ( $e \sim 10^{-6}$ ,  $\mu_T/\mu_\infty \sim 0.5$ ). The calculation has not yet been completed, but has proceeded far enough ( $tu_\infty/D \sim 0.4$ ) to observe the start of the recirculation region as a separation bubble on the base wall just below the shoulder. The wake of the boundary layer extends, at this point in the calculation, about 0.4 diameters downstream of the shoulder.

The numerical methods outlined in this report perform well, with three iterations taken to insure convergence and the results demonstrating good convergence of the rapidly changing turbulence variables after two iterations.

## 5. CONCLUSIONS

The objective of this program has been to develop the methodology for performing calculations of the near wake behind a slender body in supersonic flow. The major technical problems are the development of turbulence model equations which adequately describe a supersonic turbulent flow, and the development of numerical methods for solving these equations. A two equation model of turbulence has been developed\* which has been demonstrated to adequately predict those low and high speed turbulent flow experiments against which it has been tested. Further testing of the model is continuing as part of a separate program.

The calculation of the two-dimensional flowfield described by these two turbulence model equations and the four mean flow conservation equations has been posed, in the present study, as a time-dependent problem. The alternating-direction implicit methods developed have been demonstrated on a variety of problems of varying complexity ranging from one-dimensional shocks to the final problem of interest. The method has been shown to be especially suited to this problem because the temporal step size is not limited by the Courant criterion of explicit methods. Specifically, this permits fine spatial resolution locally without a correspondingly small time step being required. The implicit nature of the calculation also permits the description of a local equilibrium state of the turbulence properties, which can become difficult and time consuming when done explicitly because the equations can then display an instability similar to that of the stiff condition encountered in chemically reacting flows.

Results have been presented for a hypersonic laminar near wake and a turbulent calculation is well under way. The detailed results of this final calculation will be presented in an addendum to this report, to be distributed at a later time.

---

\*this work has been partially supported by ABMDA<sup>(3)</sup>

## REFERENCES

1. Ohrenberger, J. T. and Baum, E., "A Theoretical Model of the Near Wake of a Slender Body in Supersonic Flow," AIAA Journal, Vol. 10, pp. 1165-1172, 1972.
2. Semi-Annual Technical Report - Turbulent Wakes, TRW Report 23028-6001-RU-00, 30 November 1972.
3. ROPE Project Semi-Annual Report, TRW Report 18586-6001-RU-00, July 1973.
4. Baum, E. and Ndefo, E., "A Temporal ADI Computational Technique," Proceedings, AIAA Computational Fluid Dynamics Conference, pp. 133-140, July 1973.
5. Wilcox, D. and Alber, I., "A Turbulence Model for High Speed Flows," Heat Transfer and Fluid Mechanics Institute Proceedings, June 1972.
6. Bradshaw, P., Ferriss, D. H., and Atwell, N. P., "Calculation of Boundary Layer Development Using the Turbulent Energy Equations," Journal of Fluid Mechanics, Vol. 28, pp. 593-616, 1967.
7. Harlow, F. H. and Nakayama, P. I., "Turbulent Transport Equations," Physics of Fluids, Vol. 10, pp. 2323-2332, 1967.
8. Jones, W. P. and Launder, B. E., "The Prediction of Laminarization with a Two-equation Model of Turbulence," Int. Journal of Heat and Mass Transfer, Vol. 15, pp. 301-314.
9. Boris, J. P. and Book, D. L., "Flux Corrected Transport I. SHASTA, A Fluid Transport Algorithm that Works," Journal Computational Physics, Vol. 11, pp. 38-69, 1973.
10. ROPE Project Final Technical Report: Volume II-Reentry Observables, TRW Report 18586-6047-RU-00, November 1972.